measured using shear cells; while in the other, shear stresses are derived from pairs of perpendicular normal stresses measured with pressure cells. Here again the agreement between values compared is very good.

It appears that, at least for the conditions present in the homogeneous dry sand test section, the shear cell is capable of measuring shear stresses directly with a reasonable degree of accuracy.

Application of the Elastic Theory to Highway Embankments by Use of Difference Equations

J. C. DINGWALL, *Engineer of Road Design*, and
F. H. SCRIVNER, *Senior Research Engineer*
Texas Highway Department

THE problem solved in this paper by the use of the theory of elasticity consists in the determination of the shearing and normal stresses in a trapezoidal embankment and its foundation consisting of a relatively thin, uniform, natural layer which, in turn, is underlaid by a rigid boundary, such as the top surface of a rock or stiff soil deposit. It is assumed that the materials of the embankment and its foundation are characterized by identical elastic constants. Using the stress function, a series of differential equations is obtained and replaced by finite difference equations from which the stresses may be found. This is done for a numerical example in which Mohr's circle is applied to determine the values of cohesion and internal friction required to prevent an overstressed condition in the given structure.

● THE factor of safety of an embankment slope is usually computed by application of well-known methods involving the assumption of a surface of sliding along which the average shearing stress is computed from statics. Stresses in embankment foundations have been computed from the theory of elasticity by several methods, but those known to the author have failed to satisfy all boundary conditions (*1*, *2*, *3*, *4*).

Zienkiewicz (*5*) has computed the stresses within a concrete dam with proper regard for boundary conditions by the substitution of finite difference equations for the differential equations of elasticity and by using the method of successive approximations known generally as the "Method of Relaxation" (*6*) for solving the difference equations.

In the present case, it is proposed to use an attack similar to that of Zienkiewicz, but with the addition of a rigid horizontal surface at some distance beneath the surface of the ground. Such a condition frequently exists in the coastal region of Texas, where beds of soft clay or muck have been deposited on relatively firm strata existing at depths of 10 to 40 feet beneath the present ground surface.

STATEMENT OF THE PROBLEM

The elastic body of Figure 1 is bounded by the planes $x = 0$, $x = f$, $y = b$, $y = mx$, $y = c$, $y = d$, and $z = \pm\infty$. The embankment and foundation are symmetrical about the plane, $x = 0$. The distance from the embankment to the boundary, $x = f$, is indefinitely large when compared to the vertical dimension, d-c; and the state of stress at the boundary, $x = f$, is assumed to be the same, at least to the degree of accuracy to be achieved herein, as it would have been had the embankment load not been applied. The boundary, $y = d$, is completely rigid and it is assumed that no slipping occurs along that boundary. Poisson's ratio is taken as 0.5 throughout. Gravity, which is assumed to be

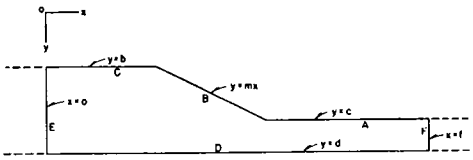

Figure 1. Half section of embankment and foundation.

the only force applied, acts in the positive direction of the y axis.

The stress in the embankment and its foundation above the rigid boundary is to be determined approximately by the substitution of finite difference equations for the differential equations of plane strain elasticity, and by the use of the method of relaxation.

GENERAL EQUATIONS APPLYING THROUGHOUT THE EMBANKMENT AND ITS FOUNDATION

Most of the symbols defined below and most of the general equations given are those used by Timoshenko (*7*).

ϕ = the Airy stress function.
σ_x = normal stress acting horizontally.
σ_y = normal stress acting vertically.
τ_{xy} = shear stress acting in planes parallel to the xz and yz planes.
u = displacement measured horizontally.
v = displacement measured vertically.
w = weight per unit of volume, assumed constant.
E = Young's modulus.

$$\sigma_x = \frac{\partial^2\phi}{\partial y^2}$$

$$\sigma_y = \frac{\partial^2\phi}{\partial x^2} - w(y - c) \qquad (1)$$

$$\tau_{xy} = -\frac{\partial^2\phi}{\partial x \partial y}$$

For Poisson's ratio equal to 0.5, Hooke's law may be written in the following form:

$$\frac{\partial u}{\partial x} = -\frac{3}{4E}\left[\frac{\partial^2\phi}{\partial x^2} - \frac{\partial^2\phi}{\partial y^2} - w(y - c)\right]$$

$$\frac{\partial v}{\partial y} = \frac{3}{4E}\left[\frac{\partial^2\phi}{\partial x^2} - \frac{\partial^2\phi}{\partial y^2} - w(y - c)\right] \qquad (2)$$

$$\frac{\partial u}{\partial y} + \frac{\partial v}{\partial x} = -\frac{3}{E}\frac{\partial^2\phi}{\partial x \partial y}$$

As well known, the stress function must satisfy the following equation:

$$\frac{\partial^4\phi}{\partial x^4} + 2\frac{\partial^4\phi}{\partial x^2 \partial y^2} + \frac{\partial^4\phi}{\partial y^4} = 0 \qquad (3)$$

BOUNDARY CONDITIONS

On Boundaries A, B, and C the stress unction and its first derivatives are known. On Boundaries D and E the stress function must satisfy two differential equations on each boundary. On Boundary F and throughout the region beyond, the stress function is given by

$$\phi = \frac{-w}{6}(y - c)^3 \qquad (4)$$

Figure 2 summarizes the boundary as well as the general equations.

FINITE DIFFERENCE APPROXIMATIONS TO DIFFERENTIAL EQUATIONS, AND THE METHOD OF RELAXATION

Figure 3 illustrates a square-mesh net formed by horizontal and vertical lines, with the boundaries of the embankment and foundation drawn thereon. The mesh length is equal to the constant, a.

Also shown in Figure 3 is a numbering system for 13 mesh points arranged in a geometrical pattern. The central point of this numbering pattern may occur at any point on the net. Difference equations based on the numbering system have been substituted for differential equations in this diagram.

Assume now that computed or estimated values of ϕ have been written at all net points in Figure 3 and that these initial values do not satisfy the difference equations. Fundamentally, the method of relaxation consists in changing the originally estimated values of ϕ, point by point, until all difference equations are satisfied, or nearly so, at every point on the net where they apply (*5*, *6*).

Decreasing the mesh size increases accuracy, and apparently any desired degree of accuracy may be obtained by making the mesh size sufficiently small.

Once the numerical values of ϕ carried on the net have been adjusted until all difference equations are satisfied (or nearly so), the stress components are computed from the

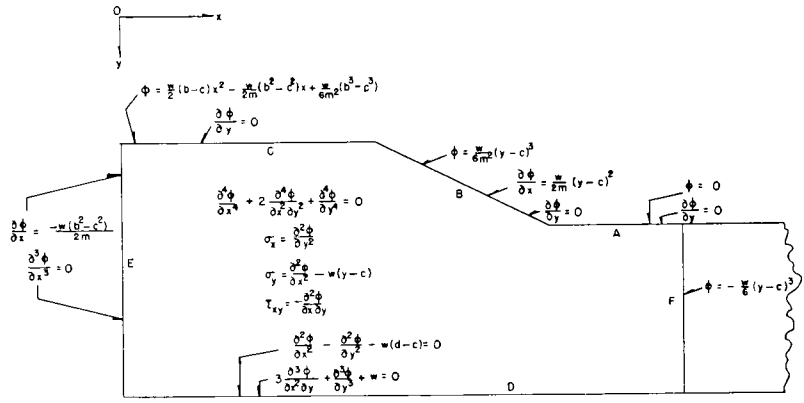

Figure 2. General and boundary equations in ϕ. (Arrows indicate where boundary equations apply.)

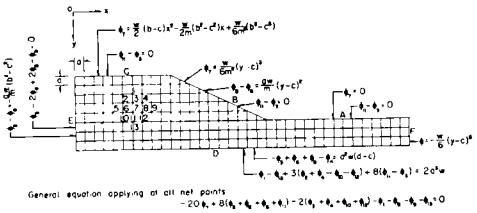

Figure 3. Algebraic and difference equations.

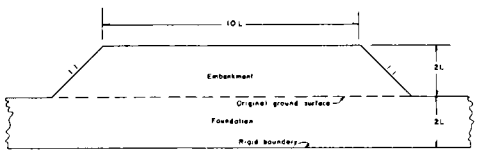

Figure 4. Shape selected for numerical solution. Results are given Figures 5, 6, 7, 8, and 9. The scale length, L, is arbitrary.

following difference equations corresponding to differential Equations 1:

$$\sigma_x \text{ at point No. } 7 = \frac{1}{a^2}(\phi_3 - 2\phi_7 + \phi_{11})$$

$$\sigma_y \text{ at point No. } 7$$

$$= \frac{1}{a^2}(\phi_6 - 2\phi_7 + \phi_8) - w(y_7 - c) \quad (5)$$

$$\tau_{xy} \text{ at point No. } 7$$

$$= \frac{-1}{4a^2}(\phi_2 - \phi_4 - \phi_{10} + \phi_{12})$$

EXAMPLE OF METHOD

Figure 4 shows the relative dimensions of an embankment with 45-deg. side slopes for which the stresses were computed by the foregoing method. The remaining figures illustrate the results of the computations in the critical area of high shear stress under the slope of the embankment.

Figure 5 gives the ratio of the maximum shearing stress (half the difference of the principal stresses) to the product, WL, where W is the density of the material and L is the

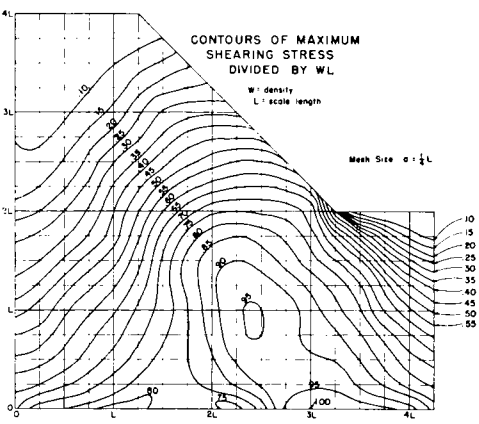

Figure 5.

scale length, which is equal to half the height of the embankment (or to one-half the thickness of the foundation layer). Examination of Figure 5 indicates that the greatest shearing stress occurs on the rigid boundary approximately under the toe of slope, and is equal to the product, WL.

As an example, consider an embankment 100 feet wide at the crown, 20 feet in height, resting on a foundation layer 20 feet thick

and underlaid by a relatively rigid material. We assume that the average density of embankment and foundation is 100 lb. per cu. ft. Then $W = 100$ and $L = 10$, and the greatest shearing stress would be $100 \times 10 = 1{,}000$ lb. per sq. ft.

Since the shear strengths of most soils increase with the average normal stress (half the sum of the principal stresses) acting on them, the normal stresses must be considered. Figure 6 shows contours of average normal stress divided by WL. It may be seen from this graph that the average normal stress at the point where the greatest shearing stress occurs is about 3.17 WL. Again taking W as 100 pcf. and L as 10 feet, we arrive at an average normal stress of 3,170 psf.

Figure 7 is a Mohr's diagram of the state of stress at the point of greatest shearing stress for the preceding example. Also plotted on this diagram is a rupture line assumed to have been determined from a triaxial test and to represent the strength of the soil. Apparently this material would not fail at the point under consideration since it clears the stress circle.

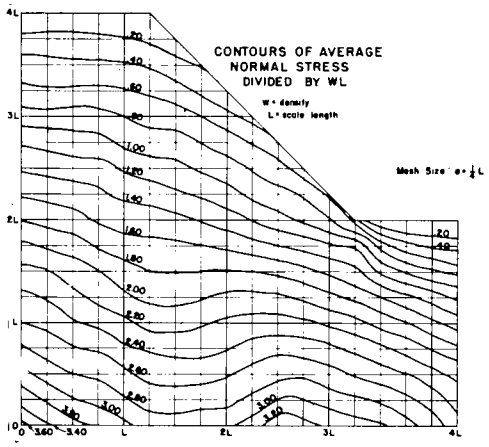

Figure 6.

STRESS ENVELOPE

However, the assumption that the soil possesses an angle of internal friction requires that additional points in the structure be investigated, provided this can be done easily. In order to facilitate comparison of strength with stress at all points within the embankment and its foundation, Figure 6 may be superimposed on Figure 5, and from the combined diagram the point of greatest shearing stress on each average normal stress contour line may be found by inspection. The pair of dimensionless values of average normal stress and maximum shearing stress at each such critical point may then be plotted as a stress circle on a Mohr's diagram. When all such circles are plotted on the same diagram, a continuous stress envelope tangent to as many circles as possible and concave downward throughout its length, may be constructed as shown in Figure 8. In comparing the strength of soils with stress, the envelope of Figure 8 may be taken to represent the stress at every critical point within the embankment and its foundation. (This concept of a stress envelope to represent the stress at every point in a plane has been used for some years in the design of flexible base in Texas.)

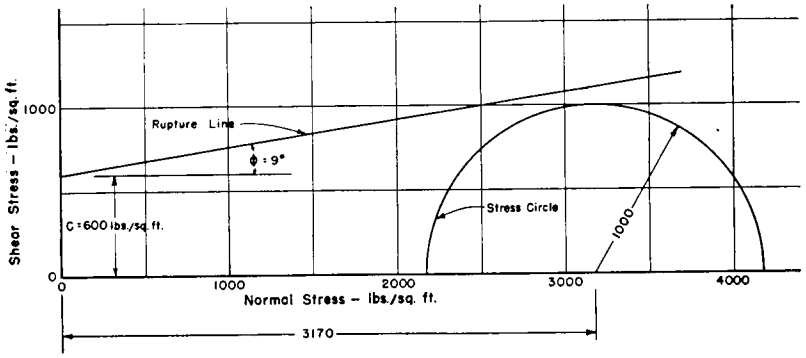

Figure 7. Mohr's diagram comparing strength of foundation with stress at point of greatest shearing stress for the case $W \times L = 1{,}000$ lb. per sq. ft.

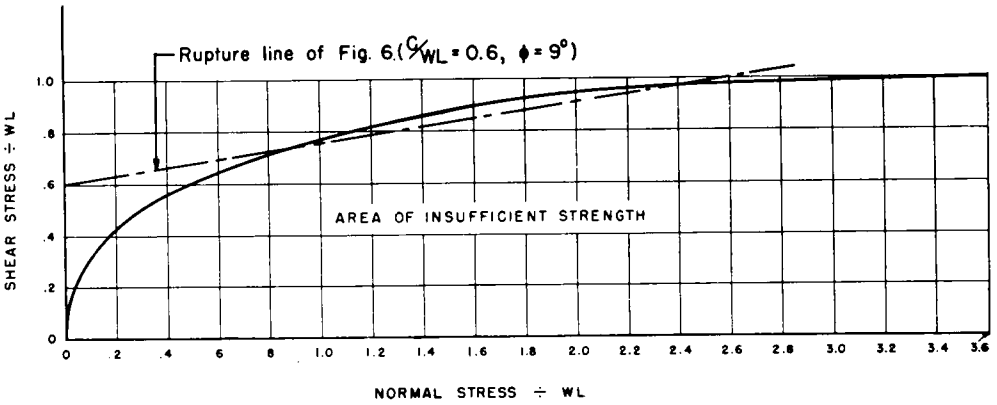

Figure 8. Envelope of critical stress circles in the embankment and foundation, for comparison with strength of soils. (Data from Figures 5 and 6.)

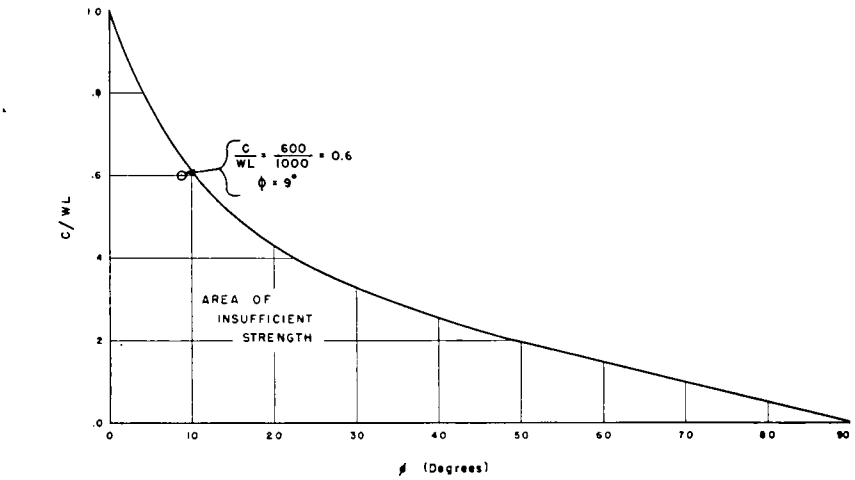

Figure 9. Cohesion and internal friction required in embankment and foundation to prevent overstress at any point. (Data from Figure 8.)

Again assuming L = 10 feet and W = 100 pcf. we may plot the rupture line of Figure 7 on Figure 8 by dividing the cohesion, C, by the product, WL, as indicated in Figure 8. Obviously, the soil would be slightly overstressed at some point in the embankment or foundation.

By drawing a series of straight-line tangents to the stress envelope of Figure 8, and measuring simultaneous values of C/WL and ϕ (representing the angle of internal friction in this case) for each tangent, the diagram of Figure 9 was constructed. The circled point in Figure 9 represents the soil in the embankment previously considered as an example.

CONCLUSIONS

At present only the problem illustrated in Figure 4 has been worked out numerically. The work was done using a desk calculator. It is hoped that a number of additional examples, treating other slopes and foundation layer thicknesses, will be completed by the IBM Computing Laboratory at A. & M. College of Texas in 1954. Meanwhile, only a few rather general conclusions can be drawn with regard to the computations presented here:

1. The use of difference equations makes possible the approximate solution of stress

problems of practical importance in soil mechanics which otherwise probably would remain unsolved.

2. For application to soil mechanics, plane stress systems generally may be reduced to a dimensionless stress envelope adequately representing the stress at every critical point in the stressed body.

3. The values of cohesion and internal friction required to prevent overstress at any point under a 1-to-1 slope (Figure 9) are apparently much greater than the values required to prevent a slide according to results obtained from the use of the sliding circle method of soil mechanics (*8*). In fact, it appears that a relatively large plastic zone may develop under the slope without danger of a slide.

4. When more numerical results, representing a variety of slopes and depths to the rigid boundary, become available, it is expected that a series of graphs of the type presented in Figure 9 can be used for quickly estimating whether a proposed design is conservative or will require a more lengthy investigation by the established methods of soil mechanics.

ACKNOWLEDGMENTS

The numerical work was accomplished with the assistance of Miss Leah Moncure, of the Texas Highway Department. L. E. McCarty, of the Texas Highway Department, and Harold J. Plass, Jr., and M. V. Barton, both of the University of Texas, furnished valuable technical assistance. D. P. Krynine, chairman of the HRB Committee on Stress Distribution in Earth Masses, made many helpful suggestions regarding the manner of presentation.

REFERENCES

1. "The Application of Theories of Elasticity and Plasticity to Foundation Problems," by LEO JURGENSON, Contributions to Soil Mechanics, 1925–1940, Boston Society of Civil Engineers, Boston, Mass., 1940, page 170.
2. "Principles of Soil Mechanics Involved in Fill Construction," by L. A. PALMER AND E. S. BARBER, Highway Research Board Proceedings, Seventeenth Annual Meeting, 1937, page 506.
3. "Drei wichtige ebene Spannungszustande des keilformigen Korpers," by P. FILLUNGER, Zeit. fur Mathematik und Physik, Leipzig, Germany, Vol. 60, 1912, pp. 275–285.
4. "Stresses and Displacements in a Semi-Infinite Elastic Body with Parabolic Cross Section Acted on by Its Own Weight Only," by R. J. HANK AND F. H. SCRIVNER, Journal of Applied Mechanics, Vol. 16, No. 2, June 1949, page 211.
5. "Classical Theories of Gravity Dam Design in the Light of Modern Analytical Methods," a thesis submitted by O. C. ZIENKIEWICZ to the University of London, 1945.
6. "Byharmonic Analysis as Applied to the Flexure and Extension of Flat Elastic Plates," by L. FOX AND R. V. SOUTHWELL, Philosophical Transactions of the Royal Society of London, No. 810, Vol. 239, Oct. 10, 1945, pp. 419–537.
7. "Theory of Elasticity" by S. TIMOSHENKO, McGraw-Hill Book Company, New York, 1934, pp. 12–26.
8. "Soil Mechanics in Engineering Practice" by KARL TERZAGHI AND RALPH B. PECK, John Wiley and Sons, New York, 1948, pp. 185–191.

APPENDIX

Derivation of the Boundary Equations Shown in Figure 2

On any horizontal boundary, $y = k$ = constant, not acted upon by external forces (such as Boundaries A and C of Figure 1), $\sigma_y = \tau_{xy} = 0$, and the following equations in ϕ apply:

$$\frac{\partial^2\phi}{\partial x \partial y} = 0$$
$$\frac{\partial^2\phi}{\partial x^2} = w(k - c) \tag{6}$$

Integrating Equations 6 along the boundary, we find for Boundary A,

$$\phi = C_1 x + C_2$$
$$\frac{\partial\phi}{\partial x} = C_1 \tag{7}$$
$$\frac{\partial\phi}{\partial y} = C_3$$

where C_1, C_2 and C_3 are constants of integration.

Similarly, for Boundary C,

$$\phi = \frac{w(b-c)}{2}x^2 + C_4 x + C_5$$

$$\frac{\partial \phi}{\partial x} = w(b-c)x + C_4 \tag{8}$$

$$\frac{\partial \phi}{\partial y} = C_6$$

where C_4, C_5 and C_6 are constants of integration.

On Boundary B, $m^2\sigma_x - m\tau_{xy} = 0$ and $\sigma_y - m\tau_{xy} = 0$. If the corresponding equations in ϕ are added and subtracted, the following equations result for Boundary B:

$$\frac{\partial^2 \phi}{\partial x^2} - m^2 \frac{\partial^2 \phi}{\partial y^2} = w(y-c)$$

$$\frac{\partial^2 \phi}{\partial x^2} + 2m \frac{\partial^2 \phi}{\partial x \partial y} + m^2 \frac{\partial^2 \phi}{\partial y^2} = w(y-c) \tag{9}$$

Since both x and y vary on Boundary B, it is convenient to transform Equations 9 to a pair of new variables so selected that one will be constant on Boundary B. The variables chosen are given below:

$$s = mx + y$$
$$t = mx - y$$

Then, on Boundary B, according to Equations 9,

$$4m^2 \frac{\partial^2 \phi}{\partial s \partial t} = w\left(\frac{s}{2} - c\right)$$

$$4m^2 \frac{\partial^2 \phi}{\partial s^2} = w\left(\frac{s}{2} - c\right) \tag{9a}$$

Integrating Equations 9a with respect to the variable, s (t being zero on B) and transforming the result to the variables, x and y, we obtain on B:

$$\phi = \frac{w}{6m^2}(y^3 - 3cy^2) + 2C_3 y + C_9$$

$$\frac{\partial \phi}{\partial x} = \frac{w}{2m}(y_2 - 2cy) + C_7 m + C_8 m \tag{10}$$

$$\frac{\partial \phi}{\partial y} = C_8 - C_7$$

where C_7, C_8 and C_9 are constants of integration.

The distribution of stress is symmetrical about Boundary E and that boundary is a principal plane in which τ_{xy} vanishes. Therefore, on Boundary E,

$$\frac{\partial^2 \phi}{\partial x \partial y} = 0 \tag{11}$$

$$\frac{\partial \sigma_y}{\partial x} = \frac{\partial^3 \phi}{\partial x^3} = 0 \tag{12}$$

By integrating Equation 11 along the boundary, we obtain on Boundary E,

$$\frac{\partial \phi}{\partial x} = C_{10} \tag{13}$$

where C_{10} is a constant of integration.

Equations 12 and 13 express the conditions on Boundary E.

On Boundary D,

$$u = 0$$
$$v = 0 \tag{14}$$

Differentiating the first of Equations 14 along the boundary and comparing with the first of equations 2, we find on Boundary D,

$$\frac{\partial^2 \phi}{\partial x^2} - \frac{\partial^2 \phi}{\partial y^2} - w(d-c) = 0 \tag{15}$$

Differentiating the second of Equations 14 along the boundary and comparing with the third of Equations 2 we find on Boundary D,

$$\frac{\partial u}{\partial y} = -\frac{3}{E}\frac{\partial^2 \phi}{\partial x \partial y} \tag{16}$$

Differentiating Equation 16 along the boundary, we find on Boundary D,

$$\frac{\partial^2 u}{\partial x \partial y} = -\frac{3}{E}\frac{\partial^3 \phi}{\partial x^2 \partial y} \tag{17}$$

By differentiating the first of Equations 2, we obtain,

$$\frac{\partial^2 u}{\partial x \partial y} = -\frac{3}{4E}\left[\frac{\partial^3 \phi}{\partial x^2 \partial y} - \frac{\partial^3 \phi}{\partial y^3} - w\right] \tag{18}$$

From Equations 17 and 18, we conclude that on Boundary D,

$$\frac{3\partial^3 \phi}{\partial x^2 \partial y} + \frac{\partial^3 \phi}{\partial y^3} + w = 0 \tag{19}$$

Equations 15 and 19 express the conditions on Boundary D.

On Boundary F and in the region, $x \geq f$, we assume the state of stress given by the following expression for ϕ:

$$\phi = -\frac{w}{6}(y-c)^3 + C_1 x + C_2 + C_3(y-c) \quad (20)$$

Equation 20 satisfies Equation 3 and the boundary conditions expressed by Equations 7, 15 and 19. The constants, C_1, C_2 and C_3, are arbitrary, since their values cannot affect the values of the stress components.

The stress function, ϕ, and its derivatives are assumed to be continuous throughout the stressed body including the boundaries. The assumption of the continuity of ϕ and its first derivatives along the boundaries furnishes the method for evaluating the constants, C_1 through C_{10}, at the intersection of F with A, A with B, B with C, and C with E. If we begin at the intersection of F with A, by arbitrarily letting $C_1 = C_2 = C_3 = 0$, and then evaluate the remaining constants at the other boundary intersections as may be appropriate, we obtain the final forms of the boundary equations shown in Figure 2.

DISCUSSION

W. C. Boyer, *Associate Professor*, and J. I. Abrams, *Research Staff Assistant, Civil Engineering Department, Johns Hopkins University*—After studying this fine paper it appears logical to appraise it from two points of view. Accordingly, comment is directed first to the solution of the problem and secondly to the results and their interpretation in the light of soil mechanics practice.

The authors have solved this problem of plane strain by utilizing the finite difference approximation for the homogeneous equation:

$$\frac{\partial^4\phi}{\partial x^4} + 2\frac{\partial^4\phi}{\partial x^2\partial y^2} + \frac{\partial^4\phi}{\partial y^4} = 0$$

Poisson's ratio was taken as 0.5 throughout for the obvious simplifications that are produced in relationships thereby. Since similar simplifications occur for the case of Poisson's ratio equal to zero, it would be of value if the authors would include this case in their future plans in order to indicate the limits of variation in the solution produced thereby.

A detailed study of this paper will make one realize the amount of work entailed in such a solution. Problems related to the purely mechanical aspects of the calculation procedure will appeal to those with specialized interest, but are not appropriate for detailed attention here. Such details have been amply covered in the literature on the subject of relaxation methods.[1]

The demonstration of boundary conditions adjacent to free surfaces, contact surfaces, surfaces of symmetry, and remote surfaces, all of which form the field of solution for the problem, provide an added insight, and many can profit from the demonstration. It may be pointed out that there is a more direct method of obtaining conditions of ϕ, the stress function, at stressed boundaries. This method[2] is discussed by Mindlin and Salvadori. The equations are derived for definitions of stress that are slightly different from those employed by the authors. However, these equations can be converted readily to the convention presented in this paper. For a simply connected region these equations become:

$$\phi_{co} = \int_0^s (B_0 l - A_0 m)\, ds$$

$$\left.\frac{\partial\phi}{\partial n}\right|_{co} = A_0 l + B_0 m$$

where:

$$A_0 = -\int_0^s \bar{y}\, ds + \int_0^s V \cdot m\, as$$

$$B_0 = \int_0^s \bar{x}\, ds$$

$$v = -w(y - c)$$

l, m—direction cosines
$\bar{x}$, $\bar{y}$—the known surface tractions
n—the normal direction

It may be verified readily that these equations yield the same boundary conditions as developed in this paper by straightforward integration. There is, of course, no essential difference in the two methods, but the method demonstrated above is economical of effort

[1] e.g. Shaw, F. S.; "An Introduction to Relaxation Method"; Dover Publications, Inc., 1953.

[2] "Experimental Stress Analysis," M. Hetenyi (Editor); Chapter 16, "Analogies," by Mindlin, R. D. and Salvadori, M. S.; pp. 752-755; John Wiley and Sons, 1950.

and reduces the development of the stress function to practically a rote procedure.

It should be pointed out that arbitrary functions may be added to ϕ and $\partial\phi/\partial n$ provided these functions do not change any stresses.

It is well to emphasize that the solution presented in this paper is applicable to 45-deg. slopes only with the added stringent conditions: (1) that the foundation soil and superimposed fill possess identical elastic properties and (2) that the problem solved has identical dimensional similarity to the solution given. These limitations point immediately to the full scope of work encompassed in providing a set of charts, as contemplated by the authors. In addition, to varying slope angles, variation in basic dimensions for each slope angle is also required. This does not resolve the additional problem of indicating variation in the solution due to values of Poisson's ratio other than 0.5.

The second part of this discussion is directed to the results presented by the authors. They have demonstrated that the maximum stress conditions throughout the stress field are encompassed by an envelope as depicted in their Figure 8. This envelope yields the necessary data to produce the curve shown in Figure 9, which may be depicted as the combinations of cohesive strength and friction angle required in the embankment and foundation to prevent overstress at any point.

It has been stated by the authors that the values given in Figure 9 "are apparently much greater than the values required to prevent a slide according to results obtained from the use of the sliding circle method of soil mechanics." This point may be emphasized by observing Figure A, which is a reproduction of Figure 9 of the paper with the ordinate scale converted to cohesive strength. Using the data[3] given by Taylor, the curve for required cohesive strength versus friction angle, for a factor of safety of one, is superimposed. Correspondingly, the curve for a factor of safety of 2 is also shown. It becomes evident that, for the case illustrated in the authors' paper, the elastic solution generally yields results indicating a factor of safety of approximately 2.5 when compared to the sliding circle method. This statement is predicated on the thought that the curves assume practical usefulness in the range of friction values between 0 deg. and 25 deg. In view of this, one may question the value of the elastic solution. The possible area of application was defined in a paper[4] by Jürgensen. He states that the overstressed points in an embankment cross section become plastic and then transmit additional stress to adjoining material. If the plastic zone is generally confined, this transfer may be effected without danger of progressive failure. The strong point of the elastic solution lies in its ability to indicate the location of the plastic zone.

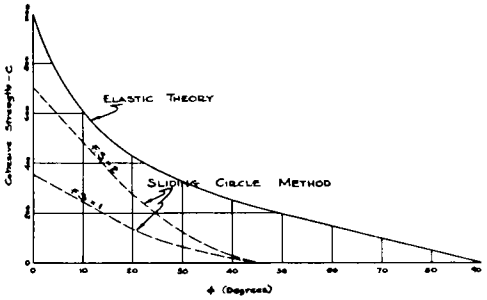

Figure A. Comparison of elastic-theory solution to sliding-circle method.

As a general rule, the plastic zone is adjacent to the toe of very steep slopes, but goes deeper into the ground as the slope flattens. In the problem illustrated in this paper it recedes and moves to the left of the toe. Below a slope of 45 deg., the probability of progressive failure is greatly lessened. Hence, a set of charts, as contemplated by the authors, should not be construed as design charts, but as the upper limiting case encompassing all possible elastic conditions of yield. Under most circumstances, the sliding circle method, with its adaptability to many effects, will suffice as a design criterion.

A limitation results from the assumption of identical elastic properties of the fill and foundation material. This condition will rarely occur in practice. It is hoped that the authors will consider this problem in extensions of their work. For their present effort, they are to be heartily congratulated.

[3] TAYLOR, D. W.; "Stability of Earth Slopes"; Journal, Boston Society of Civil Engineers; 1937; pp. 337–385.

[4] JÜRGENSEN, L.; "The Application of Theories of Elasticity and Plasticity to Foundation Problems"; Journal, Boston Society of Civil Engineers; 1937; pp. 148–182.